Receptor Site for the 5′-Phosphate of Elongator tRNAs Governs Substrate Selection by Peptidyl-tRNA Hydrolase

Michel Fromant, Pierre Plateau, Emmanuelle Schmitt, Yves Mechulam, and Sylvain Blanquet*

Laboratoire de Biochimie, UMR 7654 CNRS, Ecole Polytechnique, 91128 Palaiseau Cedex, France

Received November 9, 1998; Revised Manuscript Received January 5, 1999

ABSTRACT: Eubacterial peptidyl-tRNA hydrolase (PTH) recycles all N-blocked aminoacyl-tRNA molecules but initiator formyl-methionyl-$tRNA_f^{Met}$, the acceptor helix of which is characterized by a 1−72 mismatch. Positive selection by PTH of noninitiator tRNA molecules with a full 1−72 base pair is abolished, however, upon the removal of the 5′-phosphate. The tRNA 5′-phosphate plays therefore the role of a relay between the enzyme and the status of the 1−72 base pair. In this study, the receptor site for the 5′-phosphate of elongator peptidyl-tRNAs and the position at the surface of PTH of the 3′-end of complexed peptidyl-tRNA are identified by site-directed mutagenesis experiments. The former site comprehends two cationic side chains (K105 and R133) which are likely to clamp the phosphate. The second corresponds to a four asparagine cluster (N10, N21, N68, and N114). By using these two positional constraints, the acceptor arm of elongation factor Tu-bound Phe-$tRNA^{Phe}$ could be docked to PTH. Contacts involve the acceptor and TΨC stems. By comparing the obtained 3D model to that of EF−Tu:Phe-$tRNA^{Phe}$ crystalline complex in which the 5′-phosphate of the ligand also lies between a K and an R side chain, we propose that, in both systems, the capacity of the 5′-phosphate of a tRNA to reach or not a receptor site is the main identity element governing generic selection of elongator tRNAs. On the other hand, while the 1−72 mismatch acts as an antideterminant for PTH or EF−Tu recognition, it behaves as a positive determinant for the formylation of initiator Met-$tRNA_f^{Met}$.

Bacterial peptidyl-tRNA hydrolase recycles aborted peptidyl-tRNA molecules resulting from premature termination of translation by hydrolyzing them to free tRNA and peptide (*1*−*3*). Any N-blocked-aminoacyl-tRNA is a substrate of the hydrolase, except formyl-methionyl-$tRNA_f^{Met}$ of eubacterial origin. Indeed, formylated initiator tRNA must be kept intact to be recruited by IF2 and to participate in the formation of the ribosomal initiation complex.

Early in vitro studies with N-acyl-aminoacyl-tRNAs as substrates indicated that the action of the hydrolase was facilitated by the presence of a 5′-terminal phosphate at the end of a fully base-paired acceptor stem (*4*). This observation may explain the resistance of *Escherichia coli* formyl-methionyl-$tRNA_f^{Met}$ to cleavage by *E. coli* peptidyl-tRNA hydrolase. Indeed, like all eubacterial initiator tRNAs, *E. coli* $tRNA_f^{Met}$ lacks base pairing at position 1−72. Possibly, the resulting mismatch at the top of the acceptor helix twists the position of the phosphate group such that it can no longer trigger the activity of the enzyme. If this is true, adequate mutations in the enzyme active center capable of changing the response of the hydrolase to the presence or absence of the tRNA 5′-phosphate should be obtained. Such mutations can be searched for by assuming that, in the productive peptidyl-tRNA:enzyme complex, the 5′-phosphate of tRNA has the capacity to interact with one or several cationic amino acid side chains. The modification by site-directed mutagenesis of the charge carried by such residues should cancel the contribution of the tRNA 5′-phosphate. In the case of N-blocked-methionyl-$tRNA_f^{Met}$, the same mutations are expected neutral.

The crystal structure at 1.2 Å resolution of *E. coli* peptidyl-tRNA hydrolase was solved recently (*5*). Packing of the protein molecules in the crystal enables several main-chain atoms of three residues at the C-terminus of one peptidyl-tRNA hydrolase to establish contacts inside a channel on another peptidyl-tRNA hydrolase molecule. Such an interaction was assumed to reflect the formation of a complex between the enzyme and one product of the catalyzed reaction. At the vicinity of this channel are cationic regions possibly involved in the binding of the tRNA moiety of the substrate.

In the present study, functional probing of several residues involved in the recognition of the main-chain atoms of the peptide product was performed. A likely position of the site of hydrolysis of the ester bond of peptidyl-tRNA is deduced. To evidence the cationic side chain(s) possibly involved in the recognition of the tRNA 5′-phosphate, candidate basic side chains were selected as a function of their position with respect to the enzyme center, and single-point mutants of peptidyl-tRNA synthetase were systematically produced and assayed for their ability to cleave an *N*-acetylaminoacyl-tRNA with or without a 5′-phosphate. This approach eventually reveals one lysine (K105) and one arginine (R133) residue, the substitution of each by an alanine markedly reduces the dependence of the enzyme kinetics on the presence of the tRNA 5′-phosphate. The reduction is more pronounced with the double mutant. The two identified side

* To whom correspondence should be addressed. Phone: (33) 1 69 33 41 81. Fax: (33) 1 69 33 30 13. E-mail: blanquet@coli.polytechnique.fr.

10.1021/bi982657r CCC: $18.00
Published on Web 03/30/1999

chains are very close to each other in the 3D model of the hydrolase. They possibly offer an electrostatic clamp to interact with the 5′-terminal phosphate of elongator peptidyl-tRNAs.

MATERIALS AND METHODS

Construction and Purification of PTH Variants. Site-directed mutagenesis of the *pth* gene was performed on an M13mp19 derivative harboring this gene, as described previously (*5*). The mutated genes were completely sequenced prior to insertion into the pUC18 expression vector. Then, the resulting plasmids were used to transform the *E. coli* strain K37ΔpthTr, in which the chromosomal *pth* gene is disrupted and in which a temperature-sensitive plasmid carries a wild-type *pth* gene (*5*). For each PTH variant analyzed in the present study, the transformants succeeded in growing at a temperature (42 °C) that caused the loss of the thermosensitive plasmid. This result shows that each mutant PTH enzyme had retained enough activity to complement the absence of wild-type PTH activity. Purification of PTH variants from such transformants resulted in enzymes devoid of any contamination by wild-type PTH. Growth of the cells and purification of the mutant enzymes through Q-Sepharose and SP-Sepharose (Pharmacia) chromatographies were performed as described (*5*). According to SDS−PAGE analysis, purified PTH variants were at least 95% homogeneous.

Preparation of PTH Substrates. E. coli $tRNA_f^{Met}$ was overexpressed in strain JM101Tr (*6*) from plasmid pB-$StRNA^{fMet}_Y$ (*7*). $tRNA_{f2}^{Met}$ accepting 1700 ± 100 pmol of methionine/A_{260} unit was purified from these cells as described (*8*). Purified $tRNA_f^{Met}$ (33 nmol) was aminoacylated at 28 °C in a reaction mixture (625 μL) buffered with 20 mM Tris-HCl (pH 7.5), containing 7 mM $MgCl_2$, 150 mM KCl, 2 mM ATP, 70 μM [^{14}C]L-methionine (2.1 GBq/mmol), 10 mM 2-mercaptoethanol, and 1 μM M547 methionyl-tRNA synthetase (*9*). After a 15 min incubation, formylation was triggered by the simultaneous addition of 125 μM FTHF and 1 μM *E. coli* formylase purified as described (*10*). After a further 15 min incubation at 25 °C, the reaction was quenched by ethanol precipitation in the presence of 0.3 M sodium acetate (pH 4.8). The obtained material was incubated for 30 min in the presence of 10 mM $CuSO_4$ and chromatographied on a Chelex 100 column, as described previously (*5*). After ethanol precipitation and centrifugation, the tRNA sample was redissolved in 0.2 mL of a 20 mM sodium acetate buffer (pH 5.5) containing 100 mM KCl and 0.1 mM EDTA and applied on a Trisacryl GF05 (IBF, France) gel filtration column (10 mL) equilibrated in the same buffer. The recovered formyl-methionyl-tRNA was precipitated with ethanol and stored at −20 °C. Before use, the pellet was redissolved in 5 mM sodium acetate (pH 5.5) containing 0.1 mM EDTA.

E. coli $tRNA^{Lys}$ was produced, lysylated, acetylated, and purified on Chelex 100 as described previously (*5*). The obtained diacetyl-lysyl-tRNA sample was chromatographied on a Trisacryl GF05 column, and stored as above. The derivative of *E. coli* $tRNA_f^{Met}$ with an $A_{72}G$ change was produced as described (*8*). Dephosphorylation of $tRNA_f^{Met}$ was carried out as described previously for $tRNA^{Lys}$ (*5*).

Peptidyl-tRNA Hydrolase Assay. Peptidyl-tRNA hydrolase activity was measured at 28 °C in 100 μL assays containing 20 mM Tris-HCl (pH 7.5), 10 mM $MgCl_2$, 0.1 mM EDTA, 0.7−25 μM of the substrate under study, and catalytic amounts of PTH (0.6 nM to 4 μM). The reaction was quenched by the addition of 100 μL of 5% TCA and 20 μL of carrier RNA from yeast (4 mg/mL). The sample was centrifuged, and the released radioactivity was measured in the supernatant by scintillation counting, as described (*11*). K_m and k_{cat} values were derived from iterative nonlinear fits of the theoretical Michaelis equation to the experimental values, using the Levenberg−Marquardt algorithm. Confidence limits on the fitted values were obtained by 100 Monte Carlo simulations followed by least-squares fitting, using the experimental standard deviations on individual measurements (*12*).

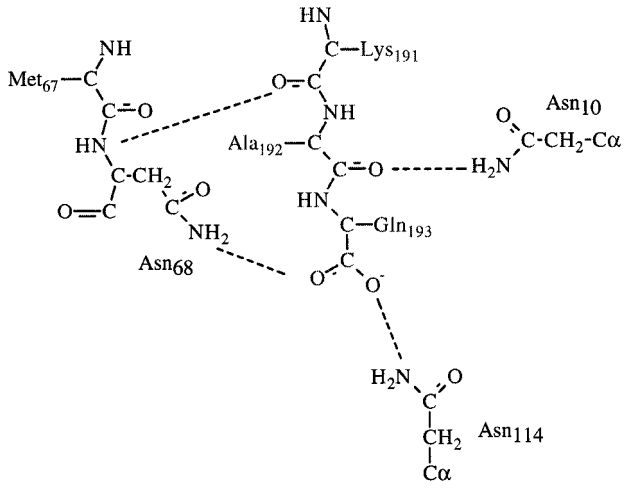

FIGURE 1: Hydrogen bonds between residues belonging to the active center of peptidyl-tRNA hydrolase and main chain atoms of the three C-terminal residues (191−193) of a neighboring enzyme molecule in the crystal. The side chains of asparagines 10, 68, and 114 are represented (hydrogen donors).

RESULTS

1. Active-Site Mapping of Peptidyl-tRNA Hydrolase Designates Its Reaction Center. In the crystal, in agreement with the expected broad specificity of PTH, the contacts between the C-end ($_{191}$KAQ$_{193}$) of one enzyme molecule and the surface of another enzyme molecule only involve main-chain atoms of the former (*5*). Electrostatic bonds occur between the free carboxylate oxygens of Q193 and the amide nitrogens of N114 and N68, between the main chain oxygen of A192 and the amide nitrogen of N10, and between the main oxygen of K191 and the main-chain nitrogen of N68. Such a network summarized in Figure 1 indicates that the PTH channel, where the C-end is stuck, has the capacity to accommodate the amide carbonyl groups and the free carboxylate of any tripeptide. An additional bond is observed between the main-chain oxygen of H188 and the hydroxyl of the Y15 side chain. This interaction possibly reflects an accessory-binding site for a peptidic moiety composed of up to six residues. Nevertheless, this interpretation is questionable because Y15 is not conserved in the available PTH sequences, in contrast with N10, N68, and N114, in which all three are strictly constant residues.

At this stage, it remains unsolved whether Q193 at the C-end of the sticked PTH molecule precisely occupies the site of the amino acid residue esterified to the 3′ ribose in

peptidyl-tRNA or whether it occupies one secondary subsite among all those covered by the peptidyl moiety. In the first case, Q193 location would coincide with that of the aminoacyl moiety of any *N*-acetyl-blocked aminoacyl-tRNA, and N114 and/or N68 can be predicted essential to the activity of PTH. Residue N10 should also be important to the cleavage of the substrate since it may be expected to interact with the oxygen of the N-blocking group, an acetyl group in the case of the model substrate diacetyl-lysyl-tRNA^{Lys}, or a formyl one in the case of initiator tRNA. On the other hand, cleavage of diacetyl-lysyl-tRNA^{Lys} should not drastically respond to a mutation of Y15. In the second case, where Q193 occupies a subsite distinct from that of the tRNA-esterified aminoacyl moiety, N10 can be predicted to not interfere with the cleavage of the model substrate.

To decide between the two situations, the three asparagine (N10, N68, and N114) were substituted by alanine in the PTH sequence. The Y15A mutation was also undertaken. The two strictly conserved residues, T18 and N21, which also belong to the putative active site region of PTH, were included in the analysis.

First, each mutant enzyme expressed from the pUC18 vector was assayed for complementation in the context of the strain K37ΔpthTr (see Materials and Methods). All mutants showed the capacity to promote the growth of the *pth* null strain. This behavior argues that the introduced mutations did not affect the overall protein folding. Second, the catalytic parameters of the PTH variants in the hydrolysis of diacetyl-lysyl-tRNA^{Lys} were compared in vitro with those of the wild-type enzyme (Table 1). Results with the N10A variant have already been obtained (*5*). Clearly, with all the studied mutants, K_m values of the substrate remain close to the value obtained with the native enzyme. This result is in agreement with the idea that the studied residues, N10, Y15, T18, N21, N68, and N114, do not significantly contribute to the stability of the enzyme−substrate complex. In ref *5*, residues M67, F66, D93, and H113, which also surround the active center of the enzyme, were changed into alanines. There again, the K_m of the substrate was insensitive to the mutations. In contrast, several categories of mutations can be distinguished at the level of the k_{cat} parameter. One set includes N10, N68, and N114 associated with reduction of k_{cat} upon alanine substitution by 2 orders of magnitude. D93 can be added to this category. Another set comprehends residues Y15, T18, F66, and H113, the substitutions of which affect the catalytic rate by a factor never exceeding 6-fold. Between these two categories is the case of the N21A variant, the k_{cat} of which is 20-fold smaller than that of wild-type PTH.

Altogether, the above results support the view of an involvement of the amide nitrogens of all three asparagine side chains, 10, 68, and 114, in the hydrolysis of diacetyl-lysyl-tRNA^{Lys}. Inside the putative active-site crevice of PTH, these side chains are very close to N21, D93, and H20, all of which also appear to participate in catalysis (*5*). Consequently, we are allowed to conclude that, in the crystal structure, Q193 of one PTH molecule bound to another PTH molecule actually designates the binding site of the amino acid residue esterified to the 3′ ribose in a peptidyl-tRNA. In agreement with this conclusion, cleavage of the model substrate is only slightly affected by the mutation of Y15.

Table 1: Catalytic Parameters of PTH Variants[a]

enzyme	k_{cat} (s^{-1})	K_m (μM)	relative k_{cat}/K_m	ratio of k_{cat}/K_m (5′-phosphate tRNA) to k_{cat}/K_m (5′−OH tRNA)[b]
WT[c]	3.6 ± 0.2	6.0 ± 0.7	100	17
N10A[c]	0.028 ± 0.002	6.6 ± 1.0	0.8	nd[d]
Y15A	0.93 ± 0.08	9.6 ± 1.3	16	17
T18A	0.67 ± 0.05	9.8 ± 1.2	11	14
R19A	0.13 ± 0.02	28 ± 6	0.77	16
H20A[c]	nm[d]	nm	<0.8	nd[d]
N21A	0.16 ± 0.01	9.5 ± 1	2.8	14
R33A	3.7 ± 0.2	5.5 ± 0.6	110	21
R35A	4.3 ± 0.3	7.9 ± 0.8	91	16
F66A[c]	0.9 ± 0.1	6.9 ± 0.9	33	nd[d]
M67A[c]	0.17 ± 0.02	4.1 ± 0.6	6.7	nd[d]
N68A	0.075 ± 0.007	12.5 ± 1.8	1	13
R82A	4.5 ± 0.3	7 ± 0.8	110	18
D93A[c]	0.05 ± 0.01	10 ± 2	0.8	nd[d]
K103A	>0.7	>40	2.7	14
K105A	>0.25	>40	1	**2.9**
H113A[c]	1.2 ± 0.2	8.8 ± 2.8	23	nd[d]
N114A	0.055 ± 0.004	4.9 ± 0.6	1.9	18
K117A	1.6 ± 0.3	21 ± 4	13	16
R133A	0.021 ± 0.002	14 ± 2	0.25	**4.7**
K142A [c]	>1.8	>30	10	12.5
K144A	3.8 ± 0.4	14 ± 2	45	15
R170A	3.5 ± 0.25	7.5 ± 0.9	78	18
R186A	2.8 ± 0.2	9.3 ± 1.1	50	15
R133A-K105A	0.008 ± 0.001	22 ± 4	0.061	**1.7**

[a] For each mutant enzyme, k_{cat}, K_m and k_{cat}/K_m values for phosphorylated diacetyl-lysyl-tRNA^{Lys} were measured as described in ref *5*. Relative k_{cat}/K_m values are shown, given an arbitrary value of 100 with the WT enzyme. k_{cat}/K_m values were also measured using dephosphorylated di-acetyl-lysyl-tRNA^{Lys} as substrate. [b] Ratio of k_{cat}/K_m values obtained for each PTH variant with 5′-phosphorylated and 5′-OH dephosphorylated diacetyl-lysyl-tRNA^{Lys}, respectively. [c] Reference *5*. [d] nm, not measurable; nd, not determined.

2. Catalytic Efficiency of Peptidyl-tRNA Hydrolase Responds to 5′-Dephosphorylation of the Substrate. Wild-type PTH was assayed with the substrate diacetyl-lysyl-tRNA^{Lys} with or without the 5′-phosphate. As shown in Table 1, k_{cat}/K_m in the reaction of hydrolysis is decreased 17-fold upon removal of the phosphate. This factor is compatible with the effect shown in ref *4*, using an acetyl-phenylalanyl-tRNA^{Phe} substrate.

Cleavage of formyl-methionyl-tRNA$_f^{Met}$ by the enzyme was also undertaken. As expected from refs *4* and *11*, we found (Table 2) that this tRNA was a poor substrate of the hydrolase as compared to fully phosphorylated N-blocked-lysyl-tRNA and that the efficiency of the enzyme did almost no more depend on the presence or absence of the 5′-phosphate.

Interestingly, the quantitative analysis conducted in the present study shows that, if deprived of phosphate, the two substrates diacetyl-lysyl-tRNA^{Lys} and formyl-methionyl-tRNA$_f^{Met}$ behave in a very similar manner, with nearly identical k_{cat}/K_m values. This behavior has to be brought together with the observation in refs *4* and *11* that f-Met-tRNA$_f^{Met}$ becomes a good substrate of PTH upon the creation of a full 1−72 Watson−Crick base pairing. Therefore, either the removal of the 5′-phosphate in diacetyl-lysyl-tRNA^{Lys} or the presence of a 1−72 mismatch in f-Met-initiator tRNA has very similar consequences on the efficiency of the hydrolase. This conclusion gives credit to the starting of the working hypothesis according to which tRNA 5′-phosphate is a functional relay between the enzyme and the status of the 1−72 base pair.

Table 2: k_{cat}/K_m Values of PTH Mutants in the Presence of 5′-Phosphorylated or 5′-OH Dephosphorylated Substrates[a]

	diacetyl-lysyl-tRNA ^{Lys}		formyl-methionyl-tRNA$_f^{Met}$		*f*-Met-G72-tRNA$_f$Met: 5′-phosphate[b]
	5′-phosphate	5′-OH	5′-phosphate	5′-OH	
WT	100	5.8	4.7	3.8	120
K105A	1	0.35	0.23	0.23	0.97
R133A	0.25	0.053	0.47	0.5	0.6
R133A-K105A	0.061	0.036	0.18	0.16	0.18

[a] Relative k_{cat}/K_m values were calculated given an arbitrary value of 100 to the result obtained with diacetyl-lysyl-tRNA^{Lys} and WT enzyme. [b] In this tRNA$_f^{Met}$ derivative, the A72 nucleotide is replaced by a G.

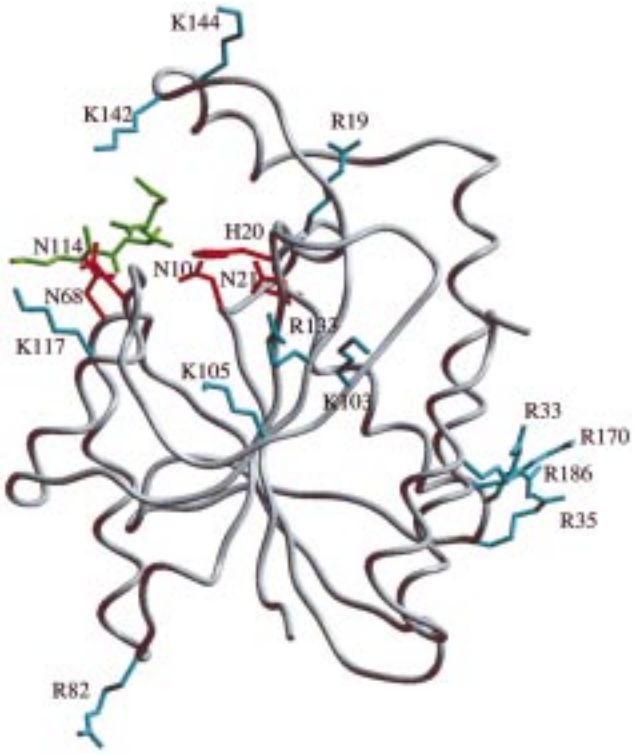

FIGURE 2: Location of the studied basic residues in the three-dimensional model of peptidyl-tRNA hydrolase. The Cα trace of the enzyme is drawn in gray. The peptidic backbone of the three C-terminal residues of a neighboring enzyme molecule in the crystal, thought to mimic the peptide product of PTH reaction, is shown with green sticks. Side chains of residues belonging to the active center are drawn in red. The blue side chains indicate the basic residues at the enzyme surface studied by site-directed mutagenesis. The figure was drawn with Setor (*21*).

3. Two Cationic Side Chains of Peptidyl-tRNA Hydrolase Are Involved in the Recognition of Elongator tRNA 5′-Phosphate. The maximum distance between the ester bond linking a peptide to tRNA and the 5′ tRNA phosphate can be measured equal to 20 Å. Assuming the active center of the hydrolase to comprehend a cluster made of N10, H20, N21, N68, D93, and N114, a sphere of radius 20 Å can be constructed from this center on the PTH 3D model. Provided that the protein is not submitted to a large structural rearrangement upon substrate binding, this sphere must contain the basic residue(s) which we suppose to interact with the 5′-phosphate at the surface of the protein. By applying this procedure, several clusters of lysine and arginine side chains exposed to the solvent appear as candidates to the binding of the tRNA phosphate (Figure 2).

The lysines and arginines of interest are mainly clustered within three areas: (i) R19, K142, K144; (ii) K103, K105, R133; and (iii) K117. All these residues were systematically changed into alanines. A few positions outside of or close to the sphere were also included in the mutagenic procedure, as controls. Chosen were R33, R35, R82, R170, and R186. Each resulting mutant enzyme was overproduced and purified after having verified that it still complemented the absence of wild-type PTH activity in vivo. The in vitro assay with diacetyl-lysyl-tRNA^{Lys} was used to compare the effects of the mutations on the michaelian parameters of the hydrolytic reaction (Table 1). In the case of the following variants, R19A, K103A, K105A, K117A, R133A, K142A and K144A, the K_m values were significantly increased with respect to that measured with the wild-type enzyme. K_m values associated to K103A, K105A, and K142A even became unmeasurable (i.e., greater than 30 μM). With R33A, R35A, R82A, R170A, and R186A, the K_m of the substrate did not change. Such a discrepancy between the behaviors of the mutant enzyme species enables the concusion that, on one hand, the negative surface potentials centered around R133, K142, and K117 can all attract the negatively charged tRNA and, on the other hand, the five arginines located far from the active center do not interfere with the productive binding of the substrate. In addition, this experiment indicates a position of the tRNA moiety on one side of the surface of the protein compatible with the orientation of the peptide product as indicated by the crystal packing. The case of R19 is peculiar because the hydrophobic part of its side chain is buried within the protein, in the vicinity of the helix which holds K142. Accordingly, the R19A mutation might cause a local structural change at the level of the helix containing K142 and affect tRNA binding indirectly. Regarding the k_{cat} values, those measured with R33A, R35A, R82A, R170A, and R186A are left roughly unchanged, in agreement with the idea that these positions do not make part of the binding area of tRNA. The rate values of all other variants are either reduced by factors lower than 15 or left unchanged (K144A) with the exception of R133A, the k_{cat} of which is lowered by 2 orders of magnitude. The whole results indicate that K103, K105, K117, R133, K142, and K144 participate to the productive binding of the substrate.

To determine if one of the above residues interacted with the 5′-end of tRNA, catalytic efficiencies of the enzyme variants were measured with either the substrate lacking the 5′-phosphate or the intact substrate (Table 1). Enzymes mutated inside the active center (Y15A, T18A, N21A, N68A, and N114A) were also included in the analysis. In most cases, the ratio between catalytic efficiencies with intact or with dephosphorylated substrate was contained between 13 and 21, very close to the ratio obtained with native peptidyl-tRNA hydrolase. The two exceptions are the R133A and K105A mutants for which the ratios between k_{cat}/K_m values

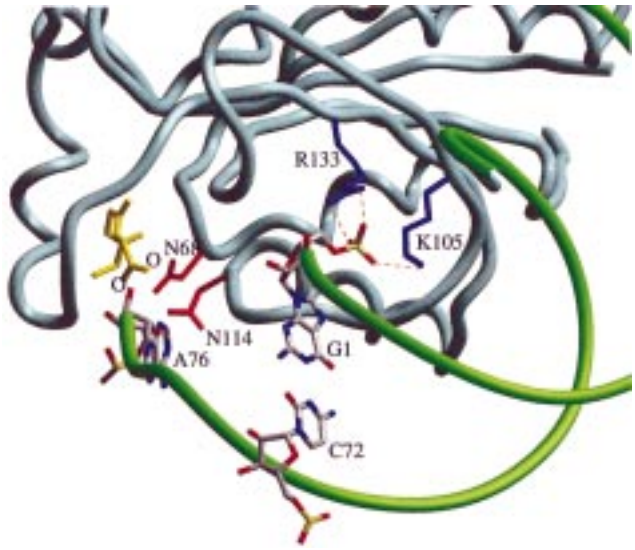

FIGURE 3: Schematic view of the proposed model for a peptidyl-tRNA hydrolase:tRNA complex. The peptidic backbone of peptidyl-tRNA hydrolase is shown in blue, with two side chains of active site residues shown in red, and the two negatively charged residues clamping the 5′-phosphate of tRNA shown in blue. Electrostatic bonds with the 5′-phosphate of tRNA are represented with red dashed lines. The green tube schematizes the backbone of the acceptor end of the docked $tRNA^{Phe}$ (see text). Bases G1, C72, and A76 are represented as sticks. The yellow sticks represent the peptidic backbone of the C-end of a neighboring enzyme molecule in the crystal with the two terminal oxygens labeled. One of these oxygens is at 1.4 Å of the 3′ OH of the ribose of A76. The figure was drawn with Setor (*21*).

become equal to 4.7 and 2.9, respectively. We conclude therefore that obliteration of the corresponding cationic side chains has made negative a large part of the positive contribution brought by the 5′-tRNA phosphate to the efficiency of catalysis. Interestingly, the two positions K105 and R133 are very close to each other on the 3D model of the hydrolase. This opened the possibility that both these residues interact with the 5′-phosphate, like a clamp. If true, the corresponding double mutant K105A−R133A should become even less sensitive to the absence of the tRNA phosphate. Table 2 shows that this is indeed the case. The ratio between the two k_{cat}/K_m values is now reduced up to a value of 1.7.

As expected, like the wild-type enzyme, K105A, R133A, and the double mutant still do not distinguish between the presence or absence of a 5′-phosphate in f-Met-$tRNA_f^{Met}$. Surprisingly, however, in the cases of the R133A and of the K105A−R133A mutants, the k_{cat}/K_m values with fmet-$tRNA_f^{Met}$ are systematically larger than those measured with dephosphorylated diacetyl-lysyl-$tRNA^{Lys}$. This discrepancy does not hold for the K105A single mutant. One possibility is that the alanine introduced instead of R133 has rendered the enzyme sensitive to some sequence feature of the substrate distinguishing between $tRNA_f^{Met}$ and $tRNA^{Lys}$, likely in the acceptor arm region. As shown in Table 2, the C_1A_{72} mismatch of $tRNA_f^{Met}$ cannot account for this effect. Authentic initiator tRNA and its derivative with an $A_{72}G$ change display the same behaviors in the presence of all mutated enzyme species assayed.

DISCUSSION

The main lesson to be drawn from this study is the occurrence at the surface of PTH of charged side chains

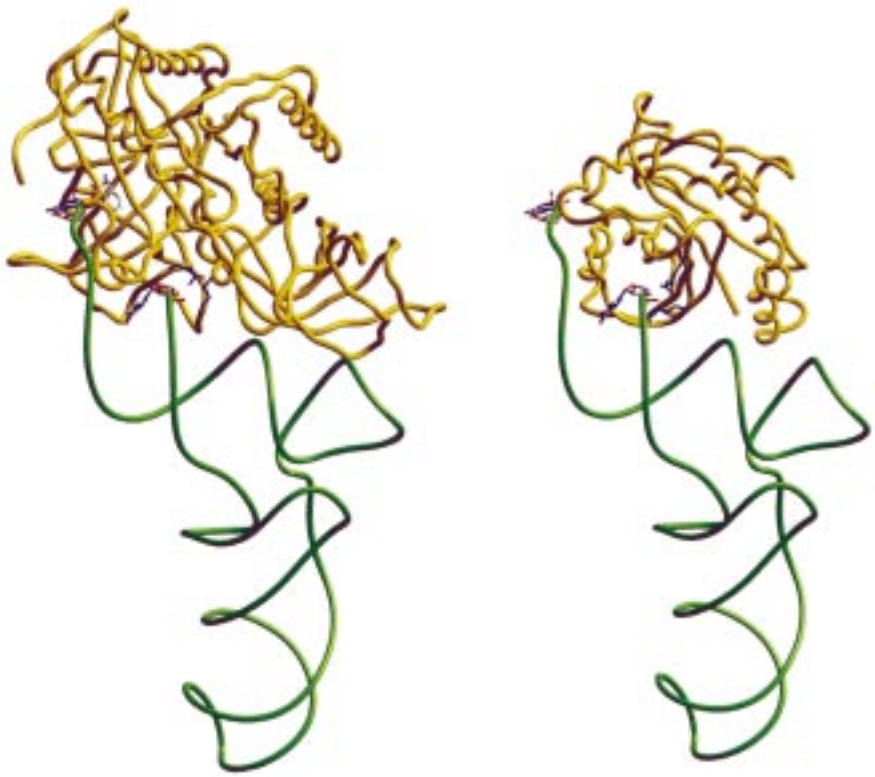

FIGURE 4: Comparison of the EF−Tu:GTP:Phe-$tRNA^{Phe}$ complex (left; *16*) with the proposed model of the peptidyl-tRNA hydrolase:$tRNA^{Phe}$ complex (right). The phosphate backbones of the bound $tRNAs^{Phe}$ are shown in green, and drawn in the same orientations. The 3′- and 5′-terminal bases are represented with sticks. Phenylalanine esterified to tRNA in also represented in the case of EF−Tu complex. The Cα traces of EF−Tu and of peptidyl-tRNA hydrolase are in yellow. The K105 and R133 side chain of PTH as well as K90 and R300 of EF−Tu are shown in blue. The figure was drawn with Setor (*21*).

capable of recognizing the 5′-phosphate of elongator peptidyl-tRNA substrates. The involvement of positively charged side chains suggests that the enzyme can directly interact with the negatively charged 5′-end of tRNA, without the need for any cofactor. This idea is in agreement with the observation in ref *5* that substrate hydrolysis by PTH can be obtained without the addition of divalent metal ions. Functional role of residues 105 and 133 in the catalytic mechanism of PTH is also indicated by the full conservation at the equivalent locations of cationic side chains in the 26 available PTH sequences of eubacterial origin, with the exception of *Borrelia burgdorferi*, the PTH of which lacks the equivalent of R133.

The above results designate K105 and R133 as receptor sites of the 5′-phosphate of tRNA. Moreover, our present site-directed mutagenesis study indicates the position of the 3′-end of complexed peptidyl-tRNA. Docking of the substrate could be therefore undertaken under these two constraints. Most of the available free or protein-complexed tRNA structures (*13*−*15*) could not be fitted simultaneously in the phosphate receptor site and in the catalytic center of the enzyme without prior rearranging of the acceptor end, in particular of the 3′-terminal adenosine. In contrast, elongation factor Tu bound Phe-tRNA^{Phe} (*16*), the 5′-phosphate of which interacts with its receptor protein, matched the constraints, and fitted at the surface of the PTH protein with very few bad contacts only involving side-chain atoms from residues involved in substrate binding such as N68, N114, and K142 (Figure 3). Such bad contacts were easily eliminated by slight motions of the corresponding side chains. In addition, the esterified amino acid in Phe-tRNA^{Phe} could be superimposed to the C-terminal residue of the mimicked PTH peptide product, without any modification of the tRNA acceptor end. The obtained model of the PTH:tRNA complex is shown on Figure 4 beside the 3D model of the EF−Tu:Phe-tRNA^{Phe} crystalline complex. In both cases, the proteins are bound to the tRNA molecules through the acceptor and TΨC stems. The position of tRNA at the surface of the PTH molecule is compatible with contacts involving K103, K105, K117, R133, and K142 (Figures 3 and 4). All these residues were shown to be important in substrate binding by site-directed mutagenesis. R33, R35, R82, and R170 remain far from the tRNA backbone. The proposed model also suggests a contact of helix α6 (residues 180−189) with the TΨC stem region. This contact is compatible with the neutrality of the R186 side chain in Michaelis complex formation, as illustrated by the data in Table 1.

In the EF−Tu.GTP:Phe-tRNA^{Phe} complex from *Thermus thermophilus* (PDB accession number 1ttt; ref *16*), the 5′-phosphate of bound Phe-tRNA^{Phe} also lies between an Arg (R300) and a Lys side chain (K90), like in the proposed model of PTH-docked tRNA. These two basic residues show a remarkable conservation among the several tenths of available EF−Tu sequences. It is therefore tempting to speculate that, in the EF−Tu system, the 5′-phosphate is again used as one generic determinant for the specific recognition of the family of elongator tRNA molecules. Actually, studies by ref *17* have shown that the presence of the 5′-phosphate at the end of a fully base-paired helix is essential for the formation of stable complexes between the bacterial elongation factor Tu and aminoacyl-tRNAs. In contrast, because of the C_1-A_{72} mismatch, exclusion of the 5′-phosphate from the receptor site on either PTH or EF−Tu would help initiator tRNA to escape removal of its formyl-methionyl moiety, on one hand, and to escape diversion from the translation initiation pathway, on the other hand. From the present study and from (*11*), an N-blocked initiator Met-tRNA can be estimated a 10−20-fold weaker substrate of PTH than an N-blocked elongator aa-tRNA. In ref *18*, the affinity of Met-tRNA$_f^{Met}$ for the elongation factor is measured 10-fold smaller than that of an aminoacylated elongator tRNA.

Interestingly, N-formylation of tRNA$_f^{Met}$-esterified methionine by Met-tRNA$_f^{Met}$ transformylase is also governed by the 1−72 mismatch (*8*, *19*, *20*). Consequently, a same defect allows the initiator tRNA to escape twice misappropriation by EF−Tu. It serves as the main positive signal for a formyl addition which strongly precludes further EF−Tu binding (*18*). Before this, the mismatch directly hinders recognition of Met-tRNA$_f^{Met}$ by the elongation factor. With the latter protein, however, like with PTH, the tRNA 5′-phosphate serves to sense the status of the 1−72 base pair.

REFERENCES

1. Kössel, H., and RajBhandary, U. L. (1968) *J. Mol. Biol. 35*, 539−560.
2. Kössel, H. (1969) *Biochim. Biophys Acta 204*, 191−202.
3. Cuzin, F., Kretchmer, N., Greenberg, R. E., Hurwitz, R., and Chapeville, F. (1967) *Proc. Natl. Acad. Sci. U.S.A. 58*, 2079−2086.
4. Schulman, L. H., and Pelka, H. (1975) *J. Biol. Chem. 250*, 542−547.
5. Schmitt, E., Mechulam, Y., Fromant, M., Plateau, P., and Blanquet, S. (1997) *EMBO J. 16*, 4760−4769.
6. Hirel, P.-H., Lévêque, F., Mellot, P., Dardel, F., Panvert, M., Mechulam, Y., and Fayat, G. (1988) *Biochimie (Paris) 70*, 773−782.
7. Meinnel, T., and Blanquet, S. (1995) *J. Biol. Chem. 270*, 15906−15914.
8. Guillon, J. M., Meinnel, T., Mechulam, Y., Lazennec, C., Blanquet, S., and Fayat, S. (1992) *J. Mol. Biol. 224*, 359−367.
9. Mellot, P., Mechulam, Y., LeCorre, D., Blanquet, S., and Fayat, G. (1989) *J. Mol. Biol. 208*, 429−443.
10. Schmitt, E., Blanquet, S., and Mechulam, Y. (1996) *EMBO J. 15*, 4749−4758.
11. Dutka, S., Meinnel, T., Lazennec, C., Mechulam, Y., and Blanquet, S. (1993) *Nucleic Acids Res. 21*, 4025−4030.
12. Dardel, F. (1994) *Comput. Appl. Biosci. 10*, 273−275.
13. Ruff, M., Krishnaswamy, S., Boeglin, M., Poterszman, A., Mitschler, A., Podjarny, A., Rees, B., Thierry, J. C., and Moras, D. (1991) *Science 252*, 1682−1689.
14. Rould, M. A., Perona, J. J., Söll, D., and Steitz, T. A. (1989) *Science 246*, 1135−1142.
15. Suddath, F. L., Quigley, G. J., McPherson, A., Sneden, D., Kim, J. J., Kim, S. H., and Rich, A. (1974) *Nature 248*, 20−24.
16. Nissen, P., Kjeldgaard, M., Thirup, S., Polekhina, G., Reshetnikova, L., Clark, B. F. C., and Nyborg, J. (1995) *Science 270*, 1464−1472.
17. Schulman, L. H., Pelka, H., and Sundari, R. M. (1974) *J. Biol. Chem. 249*, 7102−7110.
18. Janiak, F., Dell, V. A., Abrahamson, J. K., Watson, B. S., Miller, D. L., and Johnson, A. E. (1990) *Biochemistry 29*, 4268−4277.
19. Lee, C. P., Seong, B. L., and RajBhandary, U. L. (1991) *J. Biol. Chem. 266*, 18012−18017.
20. Schmitt, E., Panvert, M., Blanquet, S., and Mechulam, Y. (1998) *EMBO J. 17*, 6819−6826.
21. Evans, S. V. (1993) *J. Mol. Graphics. 11*, 134−138.

BI982657R